Current Research & Information on Pharmaceutical Sciences (CRIPS)
@NIPER, SAS Nagar, India

Research Article

Pharmacoinformatics in Identifying Potential Inhibitors of Key SARS-CoV-2 Enzymes among the Phytochemicals from *Murraya koenigii* and *Vitex negundo*

Vishnu K. Sharma[1], Prakashkumar Dobariya[2], Priyanka Kawathe[2], Abhay H. Pande[2*], Ritu Kalia[3], Mridula Singh[3], Alok Goyal[3], Sanjay M. Jachak[3], Prasad V. Bharatam[4]

[1]Department of Pharmacoinformatics, [2]Department of Biotechnology, [3]Department of Natural Products, and [4]Department of Medicinal Chemistry, National Institute of Pharmaceutical Education and Research (NIPER), Sector 67, S.A.S. Nagar (Mohali)-160062, Punjab, India,
E-mail: apande@niper.ac.in

There are several important targets which need to be explored to design and develop COVID-19 inhibitors. Several reports described the application of pharmacoinformatics in identifying natural product compounds such as tylophorine, 7-methoxycrptopleurine, scutellarein, luteolin, ferruginol, betulonic acid etc. for inhibiting the SARS-CoV-2 enzymes. However, efforts to identify species which simultaneously inhibit multiple enzyme targets are rare. In the current study, pharmacoinformatics analysis has been carried out to identify natural product inhibitors from the plant sources *Murraya koenigii* and *Vitex negundo*. The chosen SARS-CoV-2 macromolecules are 3CLpro (NSP5), PLpro (NSP3), helicase (NSP13) and endoribonuclease (NSP15). 3D Crystal structures of the target enzymes have been utilized for molecular docking-based virtual screening of phytochemicals. Lead compounds were identified based on docking scores as well as on molecular recognition interactions with the key active site residues of targeted enzymes. The results indicate that 7,8-dimethylherbacetin-3-O-αL-rhamnoside, bismahanimboline, clauraila A, mukonal, mukolidine, and mukonidine can exhibit multi-target inhibition and may provide solution to the COVID-19 treatment. Selected promising compounds were further analysed using molecular dynamics (MD) simulations to estimate the binding affinity with the target enzymes.

Introduction

Coronaviruses (CoV) are a large group of enveloped, positive-sense, single strand RNA viruses.[1,2] CoV strains that can infect humans include 229E, NL63, OC43, HKU1, SARS, MERS and SARS-CoV-2.[3] While, 229E, NL63, OC43, HKU1 infection typically lead to mild-to-moderate upper respiratory tract problems, SARS and MERS strains caused severe respiratory diseases with high morbidity and mortality. However, SARS-CoV-2 strain of CoV is highly transmissible and causes severe and fatal pneumonia.[1,4] The genome of SARS-CoV-2 is ~30 kb in length and contains (at its 5' end) a large replicase gene that occupies two-third of the entire virus genome and encodes for non-structural proteins (NSPs), structural proteins and accessory/regulatory factors.[3,5] Due to ribosomal frame shifting, the replicase gene encodes 2 open reading frames (ORFs). Consequent to the virus entry into the host cells, these two ORFs are translated into two large polyproteins (pp1a of ~490 kDa and pp1ab of ~790 kDa), which are processed auto-proteolytically by two viral proteases (PLpro between NSP 1-4 and CLpro between NSP 4-15) to generate mature 16 viral NSPs. These viral NSPs then assemble into a large, membrane-bound, replication-transcription complex, a highly dynamic protein-RNA complex responsible for facilitating the viral replicative processes. The remaining one-third genome of SARS-CoV-2 encodes for subgenomic mRNAs which get translated into four structural proteins and nine accessory/regulatory factors.[3,5] Thus, several viral SARS-CoV-2 proteins can be used as targets for inhibitor design with an aim to treat COVID-19 disease. Figure 1 and 2 provide the structures of important drugs in anti-COVID-19 research.

Clinically approved anti-viral drugs for treating viral infections caused by viruses viz. HIV, herpes, hepatitis, influenza, SARS-CoV, MERS-CoV and Ebola, are now being repurposed for treating Covid-19 disease.[6,7] Recently, remdesivir, a drug earlier approved for Ebola and favipiravir earlier used for

influenza are approved for the treatment of Covid-19 disease.[8,9] Keeping in view of limited efficacy of the clinically used drugs, it is important and timely to search for new drug candidates from natural products and traditional medicine formulations, for treating Covid-19 disease.

In Ayurveda, several medicinal herbal products are being used for the treatment and prevention of several diseases including respiratory viral infections.[10] Several of these herbs possess immune stimulating and inflammation modulating effects that help in boosting immunity and thus can offer benefits in treating respiratory viral infections. Further, many of these herbs exhibited anti-viral, anti-inflammatory and antioxidant activities that make them favourable to be considered for activity testing against Corona viruses.[11] A few Indian medicinal plant extracts of *Vitex trifolia, Spaeranthus indicus* have been reported to reduce inflammatory cytokines produced through NF-κB pathway.[12,13] This pathway has been implicated in respiratory distress induced in SARS-CoV-2 infection. *Glycyrrhiza glabra* and *Allium sativum* are known to target viral replication of SARS-CoV and may be considered as promising candidates against SARS-CoV-2.[14,15] Thus, keeping in view of potential of Indian medicinal plants we have selected *Murraya koenigii* (L.). (family: Rutaceae) and *Vitex negundo* L. (family: Verbenaceae) as potential candidates to study against SARS-COV-2 viral proteins.

Pharmacoinformatics provides information technology based tools for drug discovery.[16,17] This includes molecular modelling of proteins, small molecules and their interactions. This also involves virtual screening of large sets of data towards drug discovery applications. This technology is being extensively used in addressing the anti-virus drug discovery research including COVID-19.[18] Docking-based virtual screening (DBVS) is one of the well-known screening approaches of the structure-based drug design process.[19-21] Many attempts were made to repurpose known anti-viral compounds by initially performing pharmacoinformatic analysis.[22-24] Several studies employed virtual screening approach to identify new leads for anti COVID-19 activity.[25] Molecular docking,[26] QSAR,[27,28] Pharmacophore mapping,[29] *de novo* design,[30] Molecular dynamics,[31-33] Artificial Intelligence (AI) based analysis,[34] etc. were also carried out. A few of these efforts were carried out on a set of molecules originating from natural products also.[11,35] All these efforts lead to the identification of new hit molecules, which were occasionally submitted to molecular dynamics[31] as well as QM/MM analyses.[36]

To gain detailed insights into the structure and function of SARS-CoV-2 macromolecules, numerous 'three-dimensional' structures have been solved using

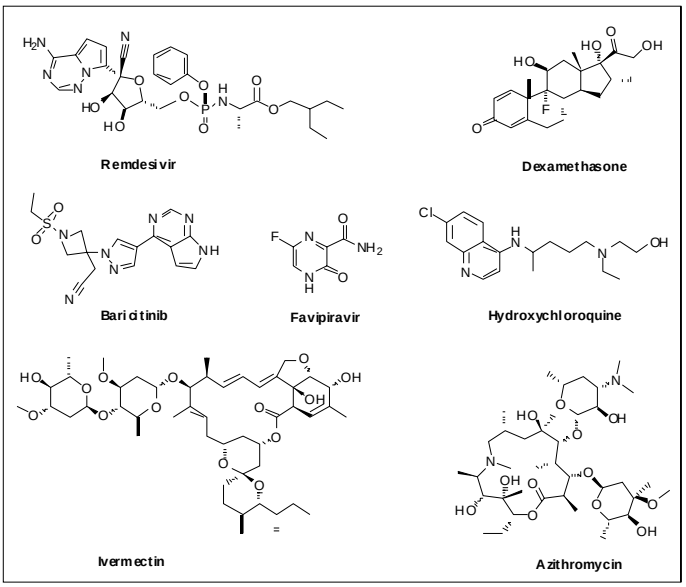

Figure 1. 2D structure of drugs currently utilized for SARS-CoV-2 treatment and approved by FDA.[37-41]

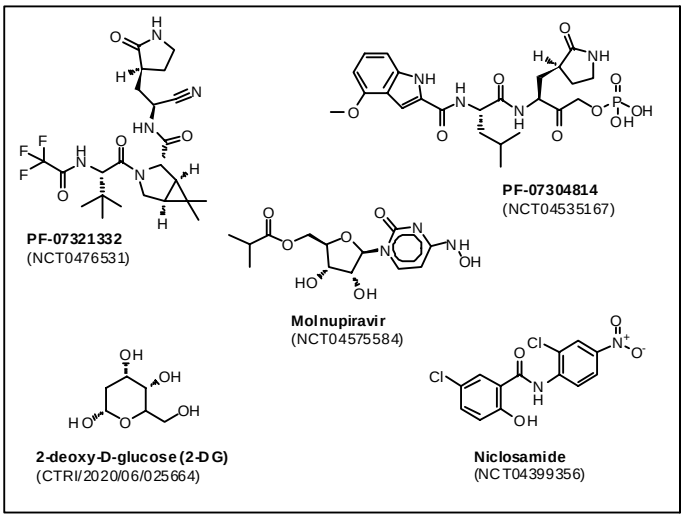

Figure 2. Drugs/molecules under clinical-trials for COVID-19 treatment.[45,46]

X-ray diffraction, solution NMR, electron microscopy techniques and deposited in the Protein Data Bank (PDB)[42] (see Table S1, ESI). Furthermore, identification of novel drugs through experimental approaches require huge money as well as time, hence, pharmacoinformatics approaches are being increasingly employed to identify new lead molecules.[16,21,43,44] There is a huge scope and emergency to explore natural product libraries towards new anti-COVID lead identification. As mentioned above, *Murraya koenigii* and *Vitex negundo* plants offer extensive set of isolatable useful phytoconstituents. It is worth exploring the possible inhibitory potential of these species against various SARS-CoV-2 enzyme targets using pharmacoinformatics methods. In this work, 265 natural products from *Murraya koenigii* and *Vitex negundo* (see Table S2, ESI) have been subjected to virtual screening analysis (Figure 3) using molecular docking. Six compounds that showed multi-

target inhibitory effects were identified, and these six compounds (Figure 4) are suggested as possible multi-target inhibitors of SARS-CoV-2. The phytoconstituents from these two species were subjected to molecular dynamics analysis (in four SARS-CoV-2 targets) to estimate the ΔG associated with the inhibitory complex formation.

METHADOLOGY

Data collection and Ligand structure preparation

The plant *Murraya koenigii* (curry tree) has been traditionally used in Indian traditional medicine for treating various ailments and holds a very high value in Ayurvedic medicine. It is also popularly known as 'Meetha neem' in India. About 200 compounds from this plant have been isolated and characterized.[47] Based on the known lead molecules for SARS-CoV-2, 98 compounds from this plant have been selected for pharmacoinformatics analysis, the 2D structure of all the molecules are provided in Table S2, ESI. *Vitex negundo* (Nirgundi) is a shrub that is reported to be an important medicinal plant used for the treatment of arthritis and several other bioactivities in Ayurveda. Around 170 isolable chemicals have been reported from this plant,[48,49] 167 of which are considered for this analysis. 2D structures of all these compounds have been collected from in-house library of natural products and corresponding 3D structures were built using ChemDraw software (version 10.0).[50] To prepare ligand(s) for molecular docking, LigPrep module of Schrödinger software[51] was utilized in which the low energy tautomeric, ionization and stereoisomeric states at physiological pH (7.0±2.0) for these molecules were generated by performing energy minimization using OPLS3e force field.[52,53]

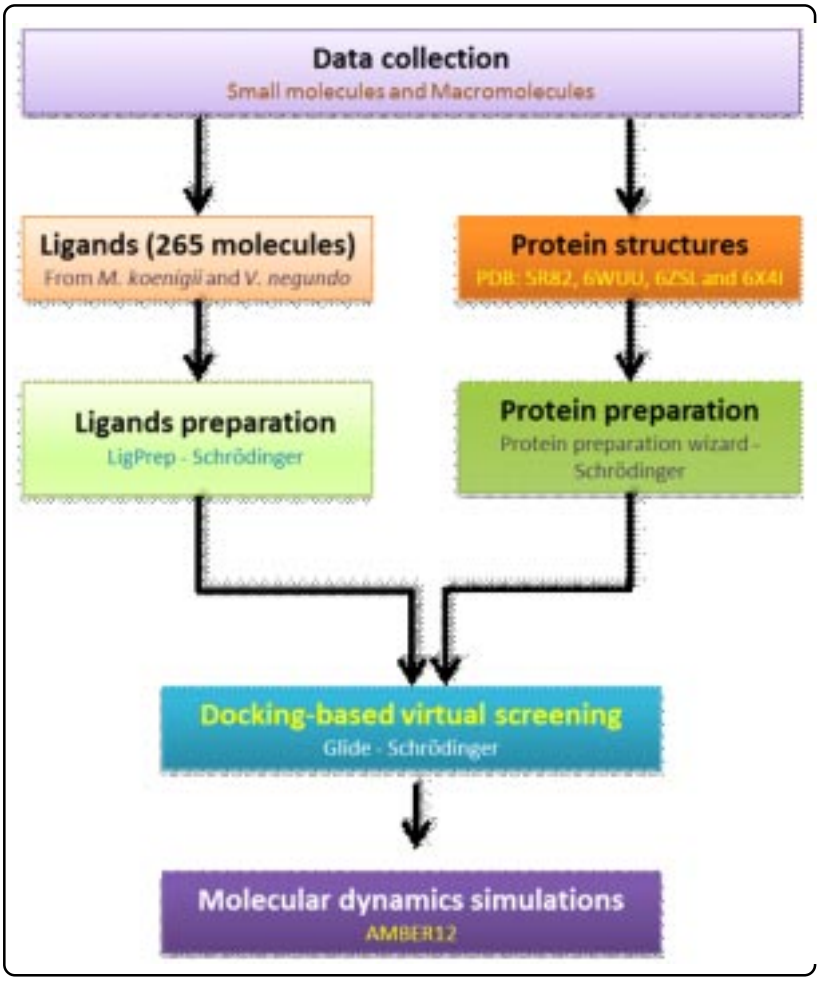

Figure 3. Flow chart of the pharmacoinformatics research reported in this study.

Molecular docking-based virtual screening

The 3D structures of the four targets were prepared for molecular docking-based screening, from the reported crystal structures available from PDB. The structures with PDB IDs: 5R82, 6WUU, 6ZSL and 6X4I have been chosen for the enzyme Main protease (Mpro/3CLpro: NSP5), Papain-like protease (PLpro: NSP3), Helicase/NTPase (NSP13) and Endoribonuclease (NendoU: NSP15) respectively. This choice is based on the resolution factors, availability of ligand bound 3D structure, andpresence of complete functional unit or domain (multiple chains, minimum missing residues etc.). The protein preparation wizard of Schrödinger software was utilized for protein structures preparation after adopting following steps.[54,55] Water molecules were removed from the downloaded 3D structures, hydrogen atoms were added. Deformities related to bond length, bond order, bond angle, metal ions, tautomers have been removed and the preferred geometric isomeric state of the amino acid side chains was restored. The ionisation state of the amino acids in these enzymes was set to pH 7±2. Out of the four proteins, two proteins lack co-crystalized ligand (bound ligand) in 3D structure. So, in order to maintain the uniformity in the docking protocol, the grid generation was done with reference to the centroid of a set of residues which contribute towards ligand binding domain. Two concentric boxes of 10x10x10 $Å^3$ (inner box) and 20x20x20 $Å^3$ (outer box) were defined to normalise the docking site for ligands.

In the final step, to validate the docking protocol, co-crystalized ligand of one of the target protein (PDB: 5R82) was docked in the defined grid. The docked ligand was very well superimposed with the co-crystalized ligand and RMSD was < 0.5 Å which confirmed that the chosen docking protocol is satisfactory. Finally, 265 phytochemicals were docked in the grid of four different protein targets of COVID19.

Final results were analysed and ranked on the basis of Glide Gscore[54] as well as on the basis of molecular recognition interactions between protein and ligand(s).

Molecular Dynamics Simulations

To validate the stability of the enzyme-ligand complex as well as ligands inside the active site of protein identified from molecular docking studies, molecular dynamics simulations were performed for the various protein-ligand complexes, using AMBER 12 package.[56] Selectivity of the ligands in various SARS-CoV-2 targets was inferred on the basis of the binding free energy contribution of the selected hits using MM-GBSA calculations, per residue energy decomposition and H-bond contributions. The Antechamber program[57] of AMBER12 software was utilized to derive partial atomic charges for the ligands using the semi-empirical (AM1) wave function with bond charge correction (BCC) model.[58] For the ligand(s) and protein(s) preparation, General Amber Force Field (GAFF)[59] and Amber ff99SB force field[60] incorporated with in AMBER12 software package were implemented, respectively to generate necessary topology and coordinate parameter files. Each of the system (complex containing protein and ligand) was solvated using TIP3P[61] water, with cubical solvation box extended to 20 Å in each direction of the solute forming a cubic box. To neutralize the overall charges of the system, Na^+ or Cl^- ions as counter ions were added to the system.

Here, to stabilize the overall protein-ligand complexes, a three step energy minimization process was adopted. In the first two steps, the solvated protein-ligand complexes were subjected to restraint minimization with 1000 and 500 minimization cycles using a force field cut-off of 3 kcal/mol/Å^2 and 1 kcal/mol/Å^2 respectively. In the third step, an unrestrained minimization upto 25000 cycles was carried out. Afterwards, under constant volume-constant temperature (NVT) conditions, the systems were gradually heated from 0 to 300 K over a period of 50 ps. In the three steps density equilibration under NPT ensemble, first 2 steps (50 ps each) with the weak restraint of 2 kcal/mol/Å^2 and 1 kcal/mol/Å^2, respectively followed by an unrestrained density equilibration of the 100 ps was carried out. The system was equilibrated on a constant pressure equilibration (NPT) for 1 ns at 300 K temperature and 1 atm pressure with pressure relaxation time of 2 ps. Finally, 50 ns production runs were performed at 300 K temperature and 1 atm pressure under NPT ensemble (cut-off distance for non-bonded interactions 12 Å). The long-range electrostatic interactions were treated with the Particle-Mesh Ewald (PME)[62] method. Coordinate trajectories were recorded after every 1ns for the whole MD simulation runs and recorded trajectories were analysed using CPPTRAJ[63] program incorporated in AMBER software to process and analyse molecular dynamics trajectory data for each complex system. Molecular Mechanics-Generalized Born Surface Area (MM-GBSA)[64] method was utilized to calculate the binding free energy for various ligands with protein/receptor for all the selected protein-ligand complexes over the last 5 ns trajectories to ensure good conformational sampling and reliable binding energy calculations. Visual Molecular Dynamics (VMD)[65] software was utilized to perform hydrogen-bond (H-bond) occupancy analysis between the ligand and active site residues.

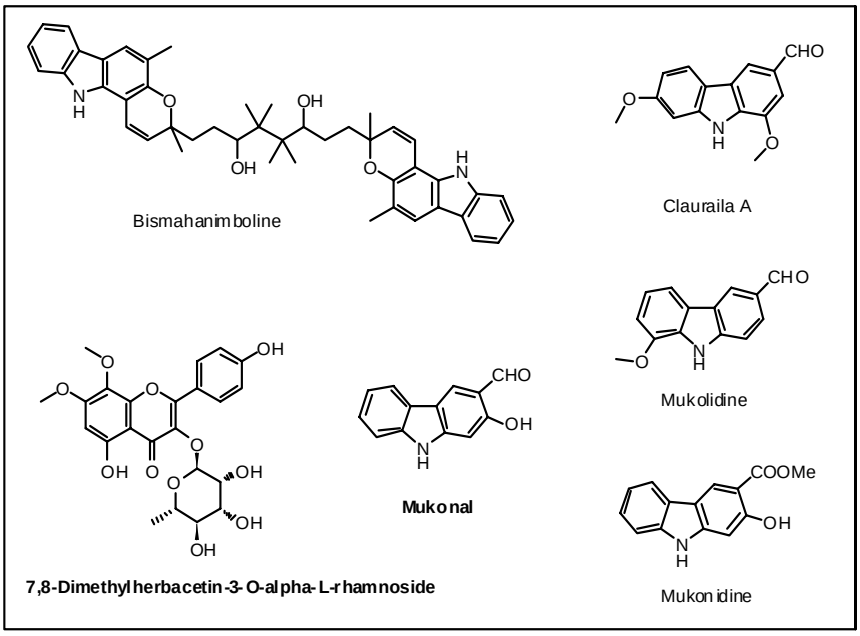

Figure 4. Suggested multi-target inhibitors for anti-COVID19 treatment. Molecules inbold forwarded for MD simulations.

RESULTS AND DISCUSSION

Molecular Docking studies to identify potential medicinal plants constituents against viral targets

An in-house phytochemicals library comprised of 265 phytoconstituents from two medicinal plants, *Murraya koenigii* and *Vitex negundo* was screened using molecular docking technique against four proven protein targets in SARS-CoV-2 determined for potent anti-COVID-19 natural compounds. Main-protease (Mpro) (also known as 3-Chymotrypsin-like protease, 3CLpro), Papain-like protease (PLpro), Helicase and Endonuclease are the non-structural proteins (NSP) vital for viral replication and therefore, most important targets for the design and development of SARS-CoV-2 inhibitors. Best 50 molecules for each protein targets were identified

on the basis of Glide Gscore (molecules which possess Glide Gscore ≤ -5 kcal/mol) as well as molecular recognizable interactions with the key active site residues of targeted proteins. These 50 molecules were also grouped according to selectivity in multiple targets (see Table S3, ESI).

Main-protease (Mpro): The main protease (Mpro) is a 306 residue protein, folded into three domains and shares ~96% sequence identity and similar 3D structure with the Mpro of other coronaviruses.[66] The enzyme plays crucial role in the coronavirus biology, Mpro is considered as "the Achilles' heel of coronaviruses". Mpro recognizes 11 conserved cleavage sites [Leu-Gln↓(Ser,Ala,Gly)] in pp1a/pp1ab polyproteins, between NSP 4-15 and is responsible for the release of NSP 4-16.[67] It is established that inhibiting the protease activity of this enzyme blocks viral replication and such inhibitors are considered as broad-spectrum anti-viral drugs. The enzyme employs conserved Cys and His residues which serve as the principal nucleophile and general acid-base catalyst, respectively, at its catalytic site.[66,68]

Molecular docking-based virtual screening of the chosen phytochemicals against Mpro revealed that most of them are accommodated comfortably in the active site. A list of top scoring 20 compounds is listed in Table 1 along with their docking scores (a comprehensive list is provided in Table S3). The top scoring five compounds are -- luteolin-7-O-β-D-glucoside (Glide Gscore -8.13), 2α,3β-7-O-methylcedrusin (-7.50), murrayacinine (-7.41), 1-hydroxy-7-methoxy-8-(3-methylbut-2-en-1-yl) -9H-carbazole-3-carbaldehyde (-7.37) and 6-hydroxy-4-(4-hydroxy-3-methoxyphenyl)-3-hydroxymethyl-7-methoxy-3,4-dihydro-2-naphthaldehyde (-7.29).

All the selected hits show single or multiple hydrogen bond interactions with the key active site residues i.e. Thr26, Asn142, Gly143, His164, Glu166, Arg188, Gln189 and Thr190. Apart from that, π-π interaction with the hydrophobic residue His41 was also observed with most of the selected hits. Hydrogen bonding with Thr25, His41, Cys44 and Leu141 also observed in selected hits (see Table S1, ESI). 7,8-Dimethylherbacetin-3-O-α-L-rhamnoside showed H-bond interaction with Asn142, Glu166 and Arg188 in which Glu166 exhibits multiple h-bond. Similarly, bismahanimboline (-6.88) showed H-bond interactions with Glu166 and Gln189 along with π-π interaction with His41. Clauraila A (-6.52) showed H-bonding with Gln189 and π-π interaction with His41. Mukonal (-6.88) exhibited H-bonding with Asn142 and Gln189 and π-π hydrophobic interaction with His41. Likewise, mukolidine (-6.73) shows a π-π interaction with His41. Mukonidine (-6.67) exhibits H-bonding with Asn142 and π-π interaction with residue His41 (see Figure 5 and Figure S1, ESI).

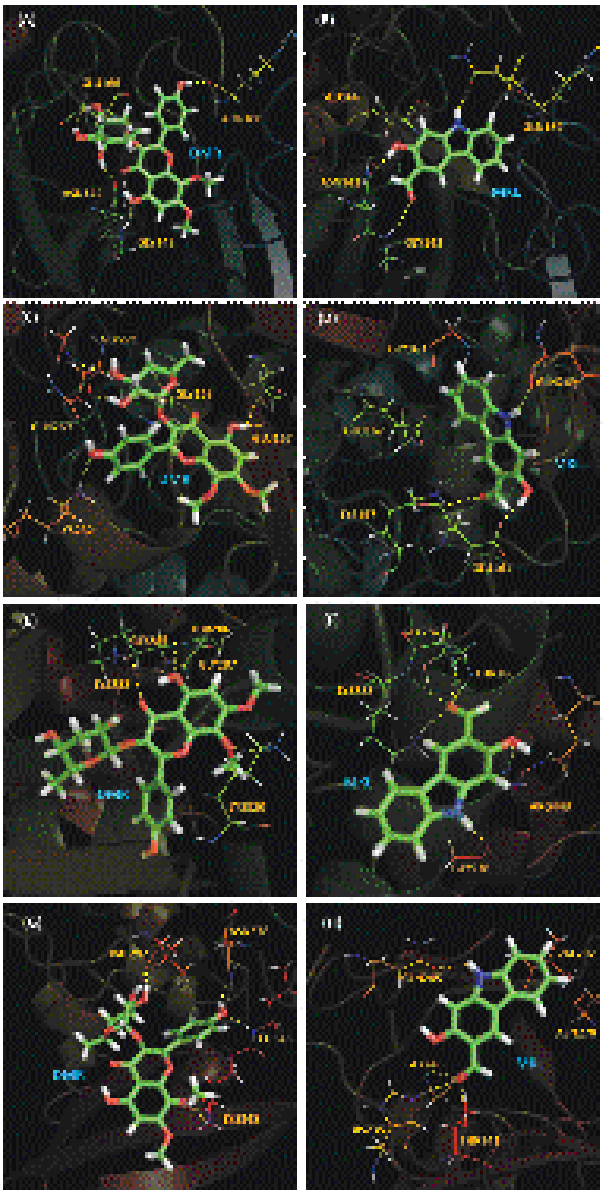

Figure 5. Molecular docking 3D structure of selected two hits in all four protein targets. (A) 5R82-DMR, (B) 5R82-MKL, (C) 6WUU-DMR, (D) 6WUU-MKL, (E) 6ZSL-DMR, (F) 6ZSL-MKL, (G) 6X4I-DMR and (H) 6X4I-MKL.

Papain-like protease enzyme: PLpro is the largest, multi-domain protein (1945 residues) produced by the SARS-Cov-2.[68,69] Mature PLpro protein is generated from pp1a/pp1ab polyproteins by autoproteolysis. PLpro acts as a scaffold protein and interacts with other viral NSP's and host proteins and plays an important role in the assembly of viral RTC (Reverse Transcription Complex).[4,66,69] The enzyme recognizes and cuts the tetrapeptide 'LxGG' motifs in pp1a and pp1ab polyproteins and releases viral NSP1, NSP2 and NSP3. Besides this, the enzyme also harbor two other activities: proteolytic removal of ubiquitin (DUB activity) and interferon-induced-gene-15 (deISG activity) from viral and host proteins.[70-72] PLpro thus plays an important role in the suppression of host innate immune responses during viral infection and helps in virus propagation

in the host.[4,66,69] Several small-molecule inhibitors of PLpro are under development.[71,73-81]

Molecular Docking-based virtual screening of PLpro revealed that the five top scoring compounds are luteolin-7-O-β-D-glucoside (-9.13), vitegnoside (-8.92), 7,8-dimethylherbacetin-3-O-α-L-rhamnoside (-8.27), 2α,3β-7-O-methylcedrusin (-8.24), and bismahanimboline (-8.09) (Table 1). All the selected hits show single or multiple hydrogen bond interactions with the key active site residues Glu161, Leu162, Gly163, Asp164, Glu167, Tyr268, and Gln269. Apart from that, Tyr171, Val202, Met206, Met208, Ile222, Tyr264, Tyr273, Thr301, and Glu203 also are involved in H-bond/π–π interaction formation with most of the selected hits (see Table S4, ESI). 7,8-dimethylherbacetin-3-O-α-L-rhamnoside (-8.27) shows H-bond interaction with Gly163, Glu167, Lys232C, Tyr264 and Gln269 along with π-cation interaction with Lys157. Similarly, bismahanimboline shows H-bond with Glu167, Pro248 and Tyr268 along with π-cation interaction with Lys157. Clauraila A shows H-bonding with Gln269 and π-π interaction with Tyr207C. Mukonal exhibits H-bonding with Glu161 and Gln269. Likewise, mukolidine shows hydrogen bonding (H-bonding) with Gln269. Mukonidine shows H-bond interaction with Gln269 (see Figure S1, ESI).

Helicase: The NTPase/Helicase of SARS-CoV-2 is a ~66 kDa (601 residues) multifunctional enzyme. The protein is folded into N-terminal Cys/His rich (CH) zinc-binding domain and a C-terminal SF1 helicase domain.[82] The enzyme exhibits multiple enzymatic activities: (a) hydrolysis of NTPs/dNTPs, (b) unwinding of DNA/RNA duplexes with 5'-3' directionality and (c) RNA 5'-triphosphatase (RTPase) activity.[83-85] During SARS-CoV-2 infection, the enzyme plays crucial role by facilitating unwinding of double-strand RNAs (produced during replication of virus in the host cells) into single strands and allowing next round of viral ss-RNA replication by RNA-dependent RNA polymerase (RdRp, NSP12). The enzyme also folds newly synthesized viral RNAs into correct secondary and tertiary structures for polyproteins translation. The RTPase activity is believed to be involved in viral mRNA capping.[82-84] Thus, viral NTPase/Helicases is an indispensable component of coronavirus replication complexes and is recognized as ideal targets for the developing antiviral drug. Many laboratories across the world are trying to develop small-molecule inhibitors of CoVNTPase/Helicase.[85-90]

The molecular docking analysis indicated that the five top ranked compounds are mukoeic acid (-7.98), 1,4α,5,7α-tetrahydro-1-β-D-glucosyl-7-(3',4'-dihydroxybenzoyl-oxymethyl)-5-ketocyclopenta[c]pyran-4-carboxylic acid (-7.89), p-hydroxybenzoic acid (-7.85), negundoside (-7.83) and salicylic acid (-7.70) (see Table S4, ESI). These selected hits exhibit interactions with the residues Gly285, Thr286, Gly287, Lys288, Ser289, Lys320, Asp374, Arg443, Gly538, Glu540 as the most common ones.

Nidoviral RNA uridylate-specific endoribonuclease (NendoU): CoV RNA uridylate-specific endoribonuclease (NendoU; NSP15) is a ~39 kDa protein (346 residues) folded into three domains: N-terminal, middle domain and C-terminal catalytic NendoU domain containing catalytic residues (His-His-Lys-Ser/Thr-Asp).[91-93] Crystal structure studies of SARS-CoV-2 NendoU revealed that monomeric protein unit forms hexamers (dimers of trimers), a corolla like super structure concentrating six independent active sites.[91] The enzyme displays an RNA endonuclease activity and can cleave both ssRNA and dsRNA (and not ssDNA/dsDNA molecules) at the 3´ of uridine and produces 2´-3´ cyclic phosphodiester and 5´-hydroxyl termini. The enzyme plays important roles in the processing of viral RNAs and is recognized as an important target for developing antiviral drug.[94,95]

Molecular docking analysis indicated that almost all the chosen chemicals get accommodated inside the active site of Nidoviral RNA uridylate-specific endoribonuclease (NendoU). The top scoring molecules are 6'-p-hydroxybenzoyl-mussaenosidic acid (-8.62), salicylic acid (-8.34), p-hydroxybenzoic acid (-8.32), mukoeic acid (-8.14) and negundoside (-8.01) are the top five scoring compounds (Table S4, ESI). The common interactions exhibited by these molecules are with the residues His235, Gly248, His250, Lys290, Val292, Thr341, Tyr343,and Leu346. Apart from that Hydrophilic/Hydrophobic interactions are also observed with amino acid residues Asn278, Cys291 and Leu346 respectively.

Common factors

Out of the 50 compounds, six molecules 7,8-dimethylherbacetin-3-O-α-L-rhamnoside, bismahanimboline, clauraila A, mukonal, mukolidine and mukonidine were common (among the top 20 scoring molecules) in all four enzyme targets (see Figure 4). These compounds showed sufficient interactions with the residues in the respective enzymes and also carry significant docking scores. Hence, these six compounds can be considered as pan enzyme inhibitors for COVID-19.

Likewise, four molecules +lyoniresinol-3α-O-β-D-glucoside, 6-hydroxy-4-(4-hydroxy-3-methoxyphenyl)-3-hydroxymethyl-7-methoxy-3,4-dihydro-2-naphthaldehyde, vitedoin A, vitexdoin F were common in 3CLpro, PLpro, and Helicase. Similarly, nine molecules 4'-O-methylmyricetin-3-O-[4"-O-β-Dgalactosyl]-β-D-galactopyranoside, 6'-p-hydroxybenzoyl mussaenosidic acid, 1,4α,5,7α-

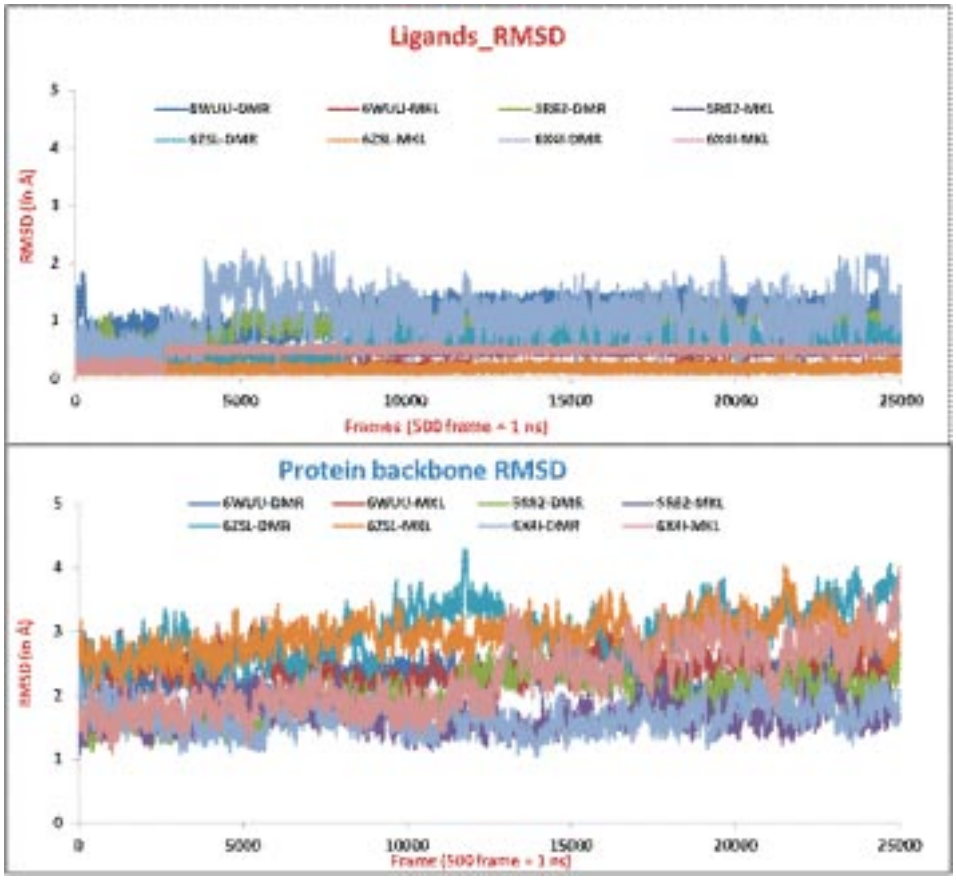

Figure 6. Ligands and protein backbone RMSD analysis of all eight binary protein-ligand complexes.

tetrahydro-1-β-D-glucosyl-7-(3',4'-dihydroxybenzoyloxymethyl) -5-ketocyclopenta[c]pyran-4-carboxylic acid, 1-hydroxy-7-methoxy-8-(3-methylbut-2-en-1-yl)-9H-carbazole-3-carbaldehyde, 3,4,5,7,3',4',5'-hexahydroxy-6,8-dimethoxyflavone, 5,7-dihydroxychromone, 5,8-dimethoxypsoralen, murrayanine and negundoside were common in 3CLpro, Helicase, and Endoribonuclease. Luteolin-7-O-β-D-glucoside and luteolin molecules were found to be common in PLpro, Helicase and Endonuclease. It was also observed that 5,3'-hydroxy-6,7,4'-trimethoxyflavone, 5,7,3'-trihydroxy-6,8,4'-trimethoxyflavone, acerosin-5-O-glucoside, iso-orientin and vitegnoside were common in PLpro, Helicase and Endonuclease. Based on the common molecules reported above, it is possible to declare lead compounds for multi-target

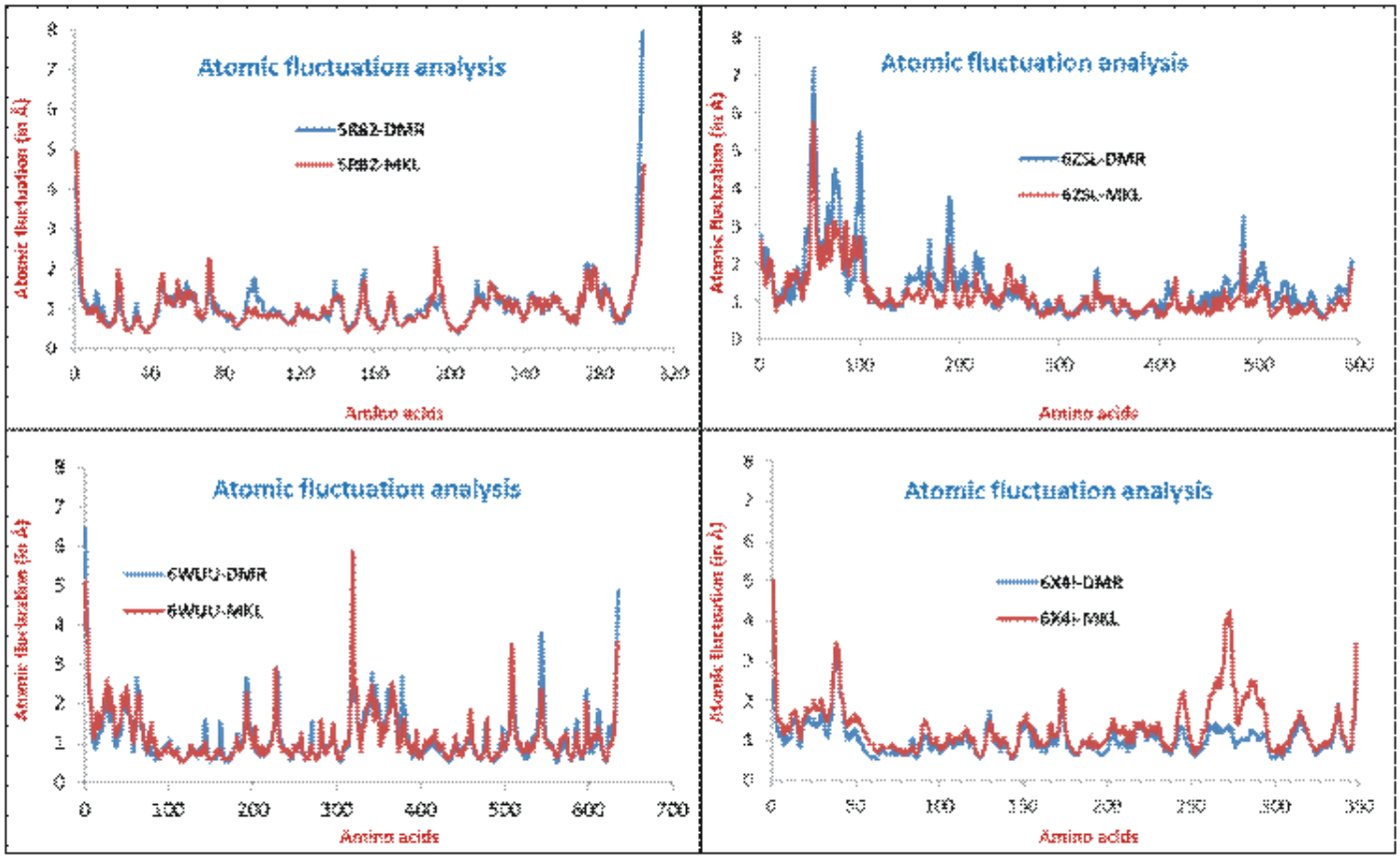

Figure 7. B-factor analysis of all eight binary protein-ligand complexes.

inhibition of COVID-19 enzymes. All the molecules maintained in this section (Table S3 and Figure S1, ESI) can be considered as lead pan inhibitors, among which molecules listed in Figure 4 are most important. To validate this, molecular dynamics simulations have been taken up, results are described in next section.

Molecular Dynamics simulation analysis

MD simulations study was explored to validate the stability of the selected hits as well as to estimate the binding affinities of the selected hits against COVID19 protein targets under the dynamic conditions. From the molecular docking exercise, best 50 molecules for each utilized target were identified. Out of 6 molecules (7,8-dimethylherbacetin-3-O-α-L-rhamnoside, bismahanimboline, clauraila A, mukonal, mukolidine and mukonidine) which are common in all four protein targets, two molecules namely 7,8-dimethylherbacetin-3-O-α-L-rhamnoside (DMR) and mukonal (MKL) have been chosen as representative of these six molecules for further molecular dynamics simulation analysis. The choice or selection of molecule is based on size (one is bigger than other one) as well as docking score in all four protein targets. Here, two binary complexes for each protein target/pdb i.e. 5R82-DMR and 5R82-MKL for 3CLpro/Mpro, 6WUU-DMR and 6WUU-MKL for PLpro, 6ZSL-DMR and 6ZSL-MKL for Helicase and 6X4I-DMR and 6X4I-MKL for NendoU, total eight binary complexes were subjected to MD simulations for 50 ns each.

The stability of all the eight binary complexes was analyzed in terms of RMSD from the initial structure. The RMSD data of whole protein complexes and protein backbones suggested that all the eight complexes get stabilized after 30 ns and the last 10 ns simulations RMSD data indicated that all the complexes maintained their stability throughout the simulations and RMSD values are in the acceptable range i.e. < 2 Å in all the eight complexes. Similarly, RMSD values of both the ligands (DMR, MKL) in all the eight binary complexes suggested that both the ligands were sufficiently stable during the simulations run and complexes were consistently stable in last 10 ns simulations run (see Figure 6 and Figure S2, S3 in ESI) and no major deviations were observed.

H-bond occupancy data of 3CLpro-ligand complex (5R82-DMR) suggested that DMR showed greater propensity to form H-bond interactions with the Leu141 (56.40%) and moderate tendency to form H-bond interaction with Cys145 (13.80%) and His163 (24.00%). Very weak H-bond formation were also observed with Ser46 (1.40%), Gly143 (3.00%), His164 (1.00%), and Glu166 (4.60%) in 5R82-DMR binary complex. In comparison to the DMR, MKL shows very weak propensity to form H-bond interaction with key active site residues. Very weak H-bond occupancy was observed in 5R82-MKL complex with Asn142 (2.80%), Gly143 (7.60%), and Glu166 (8.00%).

Similarly, H-bond occupancy data of PLpro-ligand complex (6WUU-DMR) suggested that DMR showed moderate propensity to form H-bond interactions with the main chain atoms of Gln271 (39.60%) and weak H-bond occupancies with Tyr266 (19.00%) and Tyr270 (14.60%). A very weak H-bond formation tendency was observed with Lys550 (6.80%). In comparison to the DMR, MKL shows no H-bond propensity to form H-bond interaction with any key active site residues in 6WUU-MKL complex. Likewise, H-bond occupancy data of Helicase-ligand complex (6ZSL-DMR) suggested that DMR showed greater propensity to form H-bond interactions with Ala313 (59.60%), Glu319 (45.40%) and Asp374 (88.00%) and weak tendency to form H-bond interaction with Lys320 (9.00%). Very weak H-bond formation were also observed with Ser289 (0.40%) and Ala316 (0.60%). In 6ZSL-MKL binary complex, MKL shows very weak propensity to form H-bond interaction with key active site residues. Very weak H-bond occupancy were observed with Asn142 (2.80%), Gln404 (3.00%) for MKL in 6ZSL-MKL binary complex. H-bond occupancy data of NendoU-ligand complex (6X4I-DMR) suggested that DMR showed moderate propensity to form H-bond interactions with the side chain atoms of Glu268 (21.40%) and very weak H-bond occupancies with Gln348 (0.60%). In comparison to the DMR, MKL shows no H-bond propensity to form H-bond interaction with any key active site residues in 6X4I-MKL complex.

B-factor and atomic fluctuation data of all the eight binary complexes were explored. 5R82-DMR and 5R82-MKL atomic fluctuation data revealed that there were no major fluctuations at atomic level in the 3D structure of both the complexes. Only major displacement had been seen at starting N-terminal and C-terminal end of Mpro protein. Minor atomic displacements (≤ 2 Å) were observed for residues Gln23, Ser46, Asn72, Tyr154, Asp155, Ala193, Gly215, Arg222, Gln273, Asn274 and most of these residues were part of loop regions which were far from the active site. Only Gln273 and Asn274 residues were part of α-helix which was very far from the active site.

Here, dimer of PLpro protein (chain-A and chain-C formed a dimer unit for PLpro protein) has been considered for molecular modelling study. B-factor and atomic fluctuation data of 6WUU-DMR and 6WUU-MKL revealed that there were no major fluctuations at atomic level in both the complexes. Only major displacement had been seen for initial 4 residues of N-terminal of A chain, first 5 residues of C chain and C-terminal end of C chain in PLpro protein. Minor atomic displacements (≤ 2 Å) were

observed for residues Val20A-Tyr27A, Asn60A, Thr63A, Thr191A, Thr225A, Glu1C, Thr191C, and Thr225C and most of these residues were part of loop regions which were far from the active site (see Figure7).

Table 2. MM-GBSA estimated energy values (in kcal/mol) of all eight binary complexes which were subjected to molecular dynamics analysis.

Energy Component	Protein-ligand complexes							
	5R82-DMR	5R82-MKL	6WUU-DMR	6WUU-MKL	6ZSL-DMR	6ZSL-MKL	6X4I-DMR	6X4I-MKL
E_{VDW}	-50.42	-25.39	-54.76	-21.38	-35.55	-27.32	-17.27	-20.60
E_{EL}	-40.35	-20.27	-16.59	-11.13	-71.38	-3.85	-8.06	-7.56
E_{GB}	50.40	27.41	45.62	20.75	80.20	16.60	18.64	17.98
E_{SURF}	-6.25	-3.14	-6.97	-2.92	-5.51	-3.92	-2.27	-2.61
G_{GAS}	-90.77	-45.66	-71.35	-32.51	-106.94	-31.17	-25.33	-28.15
G_{SOLV}	44.15	24.27	38.65	17.83	74.69	12.69	16.37	15.36
G_{BIND}	**-46.61**	**-21.39**	**-32.70**	**-14.68**	**-32.25**	**-18.48**	**-8.96**	**-12.79**

Likewise, B-factor and atomic fluctuation data of 6ZSL-DMR and 6ZSL-MKL revealed that major displacement had been seen between residues Asn51-Asp56, Ser74, His75, Lys76, Ser100 and Lys189 in both the binary complexes but atomic displacement were high in case of 6ZSL-DMR with respect to 6ZSL-MKL complex. Similarly B-factor and atomic fluctuation data of 6X4I-DMR and 6X4I-MKL revealed that there were no major fluctuations at atomic level in both the complexes only initial N and C terminal residues (Asn0-Ser2, Asp37, and Glu171) which are part of loop region showing major fluctuation. Apart from that, in case of 6X4I-DMR major atomic displacement at residues Ser241-Leu246, Phe259-Lys290 has been observed.

Per-residue decomposition analysis of DMR and MKL in Mpro revealed that amino acids Met49, Leu141, Gly143, Ser144, Cys145, His163, and Met165 have major contribution in the Mpro-DMR binding while Met165 major contributors for MKL binding. In the case of PLpro-DMR complex Lys157A, Leu162A, Tyr264A, Gln269A, Cys270A, and Met208C were the major contributors for binding of DMR in PLpro while Arg166C, Met206C and Met208C were the major contributors for MKL (see Figure S4, ESI). Likewise, amino acids Lys288, Ser289, His290, Ala313, Ala316 and Asp374 showed major influence for DMR binding in Helicase while Ala313, Gln537 and Gly538 majorly contributed for MKL in Helicase protein. Lys288 showed negative impact for MKL binding in Helicase. Per-residue decomposition data of Endoribonuclease-ligand complexes revealed that Cys291 and Val292 was the major contributor for DMR binding while Leu201, Gln202 and Phe259 possessed major binding contribution for MKL in Endoribonuclease-ligand complexes.

MM-GBSA analysis of all eight binary complexes revealed that molecule DMR has significant binding in all four protein targets except Endoribonuclease where molecule MKL showing greater bind for Endoribonuclease protein. Binding of MKL is comparatively low in all targeted proteins (see Table 2). It was observed that van der Waals as well as electrostatic energy contribution significantly increases binding of DMR molecule in Mpro, PLpro and Endoribonuclease. Similarly, non-polar contribution to the solvation free energy significantly increases binding affinity of DMR molecule in Mpro, PLpro and Endoribonuclease. From MM-GBSA data it become clear that, DMR is most prominent pan inhibitor for three SARS-CoV-2 protein targets Mpro, PLpro and Endoribonuclease.

CONCLUSIONS

Pharmacoinformatics techniques have been successfully utilized to identify novel inhibitors for COVID-19. Here, an attempt was made to find out some pan inhibitors which may act against multiple enzyme targets of SARS-CoV-2. Total 265 phytochemical constituents of two medicinal plants *Murraya koenigii* and *Vitex negundo* have been subjected to molecular docking-based virtual screening against four protein targets namely, Mpro, PLpro, helicase and endoribonuclease of SARS-CoV-2. Molecular docking study revealed that out of 265, six molecules have showed inhibitory effect against all four SARS-CoV-2 protein targets. These six natural compounds may be declared as pan enzyme inhibitors for COVID-19 drug discovery and development. Molecular dynamics simulations data of representative two hits suggested that 7,8-dimethylherbacetin-3-O-α-L-rhamnoside (DMR) has more binding affinity with respect to mukonal (MKL) in Mpro, PLpro and Helicase proteins while endoribonuclease shows more binding efficacy for mukonal (MKL). These molecules can be studied further as anti-COVID-19 pan inhibitors and lead molecules.

SUPPORTING INFORMATION (ESI)

The following files are available free of charge as part of supporting information (ESI).

Supporting-Information-COVID19-manuscript.pdf

REFERENCES

1. Yu J, Chai P, Ge S and Fan X 2020 Recent Understandings Toward Coronavirus Disease 2019 (COVID-19): From Bench to Bedside. Front. Cell Dev. Biol. 8 32582719
2. Velavan T P and Meyer C G 2020 The COVID-19

epidemic. Trop. Med. Int. Health 25 278
3. Docea A O, Tsatsakis A, Albulescu D, Cristea O, Zlatian O, Vinceti M, Moschos S A, Tsoukalas D, Goumenou Mand Drakoulis N 2020 A new threat from an old enemy: Re-emergence of coronavirus. Int. J. Mol. Med. 45 1631
4. Baj J, Karakula-Juchnowicz H, Teresilski G, Buszewicz G, Ciesielka M, Sitarz E, Forma A, Karakula K, Flieger W and Portincasa P 2020 COVID-19: Specific and Non-Specific Clinical Manifestations and Symptoms: The Current State of Knowledge. J. Clin. Med. 9 1753
5. Krichel B, Falke S, Hilgenfeld R, Redecke L and Uetrecht C 2020 Processing of the SARS-CoV pp1a/ab NSP7-10 region. Biochem. J. 477 1009
6. Consortium WST 2021 Repurposed Antiviral Drugs for Covid-19 - Interim WHO Solidarity Trial Results. N. Engl. J. Med. 384 497
7. Elfiky A A 2020 Anti-HCV, nucleotide inhibitors, repurposing against COVID-19. Life Sci. 248 117477
8. Altay O, Mohammadi E, Lam S, Turkez H, Boren J, Nielsen J, Uhlen M and Mardinoglu A 2020 Current status of COVID-19 therapies and drug repositioning applications. IScience 23 101303
9. Stebbing J, Phelan A, Griffin I, Tucker C, Oechsle O, Smith D and Richardson P 2020 COVID-19: Combining Anti-Viral and An Anti-Inflammatory Treatments. Lancet Infect. Dis. 20 400
10. Gyawali R, Paudel P N, Basyal D, Setzer W N, Lamichhane S, Paudel M K, Gyawali S and Khanal P 2020 A Review on Ayurvedic Medicinal Herbs as Remedial Perspective for COVID-19. JKAHS 3
11. Narkhede R R, Pise A V, Cheke R S and Shinde S D 2020 Recognition of Natural Products as Potential Inhibitors of COVID-19 Main Protease (Mpro): In-Silico Evidences. Nat. Prod. Bioprospect. 10 297
12. Matsui M, Adib-Conquy M, Coste A, Kumar-Roiné S, Pipy B, Laurent D and Pauillac S 2012 Aqueous extract of Vitex trifolia L. (Labiatae) inhibits LPS-dependent regulation of inflammatory mediators in RAW 264.7 macrophages through inhibition of Nuclear Factor kappa B translocation and expression. J. Ethnopharmacol. 143 24
13. Srivastava R A K, Mistry S and Sharma S 2015 A novel anti-inflammatory natural product from Sphaeranthus indicus inhibits expression of VCAM1 and ICAM1, and slows atherosclerosis progression independent of lipid changes. J. Nutr. Metab. 12 1
14. Vellingiri B, Jayaramayya K, Iyer M, Narayanasamy A, Govindasamy V, Giridharan B, Ganesan S, Venugopal A, Venkatesan D and Ganesan H 2020 COVID-19: A promising cure for the global panic. Sci. Total Environ. 725 138277
15. Mani J S, Johnson J B, Steel J C, Broszczak D A, Neilsen P M, Walsh K B and Naiker M 2020 Natural product-derived phytochemicals as potential agents against coronaviruses: A review. Virus Res. 197989
16. Khan D A, Hamdani S D A, Iftikhar S, Malik S Z, Zaidi N-u-SS, Gul A, Babar M M, Ozturk M, Turkyilmaz Unal B and Gonenc T 2021 Pharmacoinformatics approaches in the discovery of drug-like antimicrobials of plant origin. J. Biomol. Struct. Dyn. 40 7612
17. Bharatam P V 2003 Pharmacoinformatics: IT solutions for drug discovery and development. CRIPS 2
18. Gahlawat A, Kumar N, Kumar R, Sandhu H, Singh I P, Singh S, Sjostedt A and Garg P 2020 Structure-Based Virtual Screening to Discover Potential Lead Molecules for the SARS-CoV-2 Main Protease. J. Chem. Inf. Model. 60 5781
19. Bissantz C, Folkers G and Rognan D 2000 Protein-Based Virtual Screening of Chemical Databases. 1. Evaluation of Different Docking/Scoring Combinations. J. Med. Chem. 43 4759
20. Lyne P D 2002 Structure-based virtual screening: an overview. Drug Discov. Today 7 1047
21. Bharatam P V, Khanna S and Francis S M 2010 Modeling and informatics in drug design. Pharmaceutical Sciences Encyclopedia: Drug Discovery, Development, and Manufacturing. 1
22. Dotolo S, Marabotti A, Facchiano A and Tagliaferri R 2021 A review on drug repurposing applicable to COVID-19. Brief. Bioinformatics 22 726
23. Kandeel M and Al-Nazawi M 2020 Virtual screening and repurposing of FDA approved drugs against COVID-19 main protease. Life Sci. 251 117627
24. Shah B, Modi P and Sagar S R 2020 In silico studies on therapeutic agents for COVID-19: Drug repurposing approach. Life Sci. 252 117652
25. Kumar A, Kumar D, Kumar R, Singh P, Chandra R and Kumari K 2022 DFT and docking studies of designed conjugates of noscapines & repurposing drugs: promising inhibitors of main protease of SARS-CoV-2 and falcipan-2. J. Biomol. Struct. Dyn. 40 2600
26. Morris G M and Lim-Wilby M 2008 Molecular docking. Molecular modeling of proteins. Humana Press 443 365
27. Cherkasov A, Muratov E N, Fourches D, Varnek A, Baskin I I, Cronin M, Dearden J, Gramatica P, Martin Y C, Todeschini R and Consonni V 2014 QSAR modeling: where have you been? Where are you going to? J. Med. Chem. 57 4977
28. Tropsha A 2010 Best practices for QSAR model development, validation, and exploitation. Mol. Inform. 29 476
29. Yang S Y 2010 Pharmacophore modeling and applications in drug discovery: challenges and recent advances. Drug Discov. Today 15 444
30. Schneider G and Fechner U 2005 Computer-based de novo design of drug-like molecules. Nat. Rev. Drug Discov. 4 649
31. Karplus M and Petsko G A 1990 Molecular dynamics simulations in biology. Nature 347 631
32. Sharma V K and Bharatam P V 2021 Identification of selective inhibitors of LdDHFR enzyme using pharmacoinformatic methods. J Comput. Biol. 28 43
33. Sharma V K, Kathuria D and Bharatam P V 2021 Identification of selective LdDHFR inhibitors using quantum chemical and molecular modeling approach. J. Biomol. Struct. Dyn. 1 33904374
34. Vishnoi S, Matre H, Garg P and Pandey S K 2020 Artificial intelligence and machine learning for protein toxicity prediction using proteomics data. Chem. Biol. Drug Des. 96 902
35. Sharma V K, Nandekar P P, Sangamwar A, Pérez-Sánchez H and Agarwal SM 2016 Structure guided design and binding analysis of EGFR inhibiting analogues of erlotinib and AEE788 using ensemble docking, molecular dynamics and MM-GBSA. RSC Adv. 6 65725
36. Abbat S, Jaladanki C K and Bharatam P V 2019 Exploring

PfDHFR reaction surface: A combined molecular dynamics and QM/MM analysis. J. Mol. Graph. 87 76
37. Mei M and Tan X 2021 Current Strategies of Antiviral Drug Discovery for COVID-19. Mol. Front. J. 8 310
38. Calabrese LH and Calabrese C 2021 Baricitinib and dexamethasone for hospitalized patients with COVID-19. Cleve. Clin. J. Med. 10
39. Gasmi A, Peana M, Noor S, Lysiuk R, Menzel A, Benahmed A G and Bjørklund G 2021 Chloroquine and hydroxychloroquine in the treatment of COVID-19: the never-ending story. Appl. Microbiol. Biotechnol. 105 1333
40. Gautret P, Lagier J-C, Parola P, Meddeb L, Mailhe M, Doudier B, Courjon J, Giordanengo V, Vieira V E and Dupont H T 2020 Hydroxychloroquine and azithromycin as a treatment of COVID-19: results of an open-label non-randomized clinical trial. Int. J. Antimicrob. 56 105949
41. Gupta D, Sahoo A K and Singh A 2020 Ivermectin: potential candidate for the treatment of Covid 19. Braz. J. Infect. Dis. 24 369
42. Sussman J L, Lin D, Jiang J, Manning N O, Prilusky J, Ritter O and Abola E E 1998 Protein Data Bank (PDB): database of three-dimensional structural information of biological macromolecules. Acta Crystallogr. D 54 1078
43. Bharatam P V, Patel D, Adane L, Mittal A and Sundriyal S 2007 Modeling and Informatics in Designing Anti-Diabetic Agents. Curr. Pharm. Des. 13 3518
44. Sharma V K, Abbat S and Bharatam P V 2017 Pharmacoinformatic Study on the Selective Inhibition of the Protozoan Dihydrofolate Reductase Enzymes. Mol. Inform. 36 1600156
45. http://ctri.nic.in/Clinicaltrials/showallp.php?mid1=44369&EncHid=&userName=2-deoxy-D-glucose
46. https://clinicaltrials.gov/ct2/results?cond=COVID-19
47. Balakrishnan R, Vijayraja D, Jo S H, Ganesan P, Su-Kim I and Choi D K 2020 Medicinal Profile, Phytochemistry, and Pharmacological Activities of Murraya koenigii and its Primary Bioactive Compounds. Antioxidants 9 101
48. Singh V, Dayal R and Bartley J P 1999 Volatile constituents of Vitex negundo leaves. Planta Med. 65 580
49. Zheng C J, Li H Q, Ren S C, Xu C L, Rahman K, Qin L P and Sun Y H 2015 Phytochemical and pharmacological profile of Vitex negundo. Phytother. Res. 29 633
50. Li Z, Wan H, Shi Y and Ouyang P 2004 Personal experience with four kinds of chemical structure drawing software: review on ChemDraw, ChemWindow, ISIS/Draw, and ChemSketch. J. Chem. Inf. Comput. Sci. 44 1886
51. LigPrep, Schrödinger, LLC, New York, NY, 2021
52. Harder E, Damm W, Maple J, Wu C, Reboul M, Xiang J Y, Wang L, Lupyan D, Dahlgren M K, Knight J L and Kaus J W 2016 OPLS3: a force field providing broad coverage of drug-like small molecules and proteins. J. Chem. Theory Comput. 12 281
53. Roos K, Wu C, Damm W, Reboul M, Stevenson J M, Lu C, Dahlgren M K, Mondal S, Chen W, Wang L and Abel R 2019 OPLS3e: Extending force field coverage for drug-like small molecules. J. Chem. Theory Comput. 15 1863
54. Friesner R A, Banks J L, Murphy R B, Halgren T A, Klicic J J, Mainz D T, Repasky M P, Knoll E H, Shelley M, Perry J K and Shaw D E 2004 Glide: a new approach for rapid, accurate docking and scoring 1. Method and assessment of docking accuracy. J. Med. Chem. 47 1739
55. Glide, Schrödinger, LLC, New York, NY, 2021
56. Case D, Darden T, Cheatham T, Simmerling C, Wang J, Duke R, Luo R, Crowley M, Walker R and Zhang W 2012 AMBER 12 University of California. San Francisco 1
57. Wang J, Wang W, Kollman P A and Case D A 2001 Antechamber: an accessory software package for molecular mechanical calculations. J. Am. Chem. Soc. 222 U403
58. Jakalian A, Bush B L, Jack D Band Bayly C I 2000 Fast efficient generation of high-quality atomic charges AM1-BCC model: I. Method. J. Comput. Chem. 21 132
59. Wang J, Wolf R M, Caldwell J W, Kollman P A and Case D A 2004 Development and testing of a general amber force field. J. Comput. Chem. 25 1157
60. Lindorff-Larsen K, Piana S, Palmo K, Maragakis P, Klepeis J L, Dror R O and Shaw D E 2010 Improved side-chain torsion potentials for the Amber ff99SB protein force field. Proteins: Struct. Funct. Genet. 78 1950
61. Mark P and Nilsson L 2001 Structure and dynamics of the TIP3P, SPC, and SPC/E water models at 298 K. J. Phys. Chem. A. 105 9954
62. Darden T, York D and Pedersen L 1993 Particle mesh Ewald: An N. log (N) method for Ewald sums in large systems. J. Chem. Phys. 98 10089
63. Roe D R and Cheatham III T E 2013 PTRAJ and CPPTRAJ software for processing and analysis of molecular dynamics trajectory data. J. Chem. Theory Comput. 9 3084
64. Kollman P A, Massova I, Reyes C, Kuhn B, Huo S, Chong L, Lee M, Lee T, Duan Y and Wang W 2000 Calculating structures and free energies of complex molecules: combining molecular mechanics and continuum models. Acc. Chem. Res. 33 889
65. Humphrey W, Dalke A and Schulten K 1996 VMD: visual molecular dynamics. J. Mol. Graph. 14 33
66. Wang L, Hu W and Fan C 2020 Protein Science Structural and biochemical characterization of SARS-CoV papain-like protease 2. Protein Sci. 29 1228
67. Zhang L, Lin D, Sun X, Curth U, Drosten C, Sauerhering L, Becker S, Rox K and Hilgenfeld R 2020 Crystal structure of SARS-CoV-2 main protease provides a basis for design of improved α-ketoamide inhibitors. Science 368 409
68. Wang H, He S, Deng W, Zhang Y, Li G, Sun J, Zhao W, Guo Y, Yin Zand Li D 2020 Comprehensive Insights into the Catalytic Mechanism of Middle East Respiratory Syndrome 3C-Like Protease and Severe Acute Respiratory Syndrome 3C-Like Protease. ACS Catal. 10 5871
69. Clemente V, D'arcy P and Bazzaro M 2020 Deubiquitinating enzymes in coronaviruses and possible therapeutic opportunities for COVID-19. Int. J. Mol. Sci. 21 3492
70. Freitas B T, Durie I A, Murray J, Longo J E, Miller H C, Crich D, Hogan R J, Tripp R A and Pegan S D 2020 Characterization and Noncovalent Inhibition of the Deubiquitinase and deISGylase Activity of SARS-CoV-2 Papain-Like Protease. ACS Infect. Dis. 6 2099
71. Rut W, Lv Z, Zmudzinski M, Patchett S, Nayak D, Snipas

S J, EIOualid F, Huang T T, Bekes M and Drag M 2020 Activity profiling and structures of inhibitor-bound SARS-CoV-2 PLpro protease provides a framework for anti-COVID-19 drug design. biorxiv 32511411

72. Clasman J R,Everett R K, Srinivasan K and Mesecar A D 2020 Decoupling deISGylating and deubiquitinating activities of the MERS virus papain-like protease. Antiviral Res. 174 104661
73. Bestle D, Heindl M R, Limburg H, Pilgram O, Moulton H, Stein D A, Hardes K, Eickmann M, Dolnik O and Rohde C 2020 TMPRSS2 and furin are both essential for proteolytic activation of SARS-CoV-2 in human airway cells. Life Sci. Alliance 3 32703818
74. Gurung A B, Ali M A, Lee J, Farah M A and Al-Anazi K M 2020 Unravelling lead antiviral phytochemicals for the inhibition of SARS-CoV-2 Mpro enzyme through in silico approach. Life Sci. 255 117831
75. Chu HF, Chen CC, Moses D C, Chen YH, Lin CH, Tsai YC and Chou CY 2018 Porcine epidemic diarrhea virus papain-like protease 2 can be noncompetitively inhibited by 6-thioguanine. Antiviral Res. 158 199
76. Park JY, Yuk H J, Ryu H W, Lim S H, Kim K S, Park K H, Ryu Y B and Lee W S 2017 Evaluation of polyphenols from Broussonetia papyrifera as coronavirus protease inhibitors. J. Enzyme Inhib. Med. Chem. 32 504
77. Lee H, Lei H, Santarsiero B D, Gatuz J L, Cao S, Rice A J, Patel K, Szypulinski M Z, Ojeda I and Ghosh A K 2015 Inhibitor recognition specificity of MERS-CoV papain-like protease may differ from that of SARS-CoV. ACS Chem. Biol. 10 1456
78. Kim D W, Seo K H, Curtis-Long M J, Oh K Y, Oh JW, Cho J K, Lee K H and Park K H 2014 Phenolic phytochemical displaying SARS-CoV papain-like protease inhibition from the seeds of Psoralea corylifolia. J. Enzyme Inhib. Med. Chem. 29 59
79. Cho J K, Curtis-Long M J, Lee K H, Kim D W, Ryu H W, Yuk H J and Park K H 2013 Geranylated flavonoids displaying SARS-CoV papain-like protease inhibition from the fruits of Paulownia tomentosa. Bioorg. Med. Chem. 21 3051
80. Song Y H, Kim D W, Curtis-Long M J, Yuk H J, Wang Y, Zhuang N, Lee K H, Jeon K S, Park K H 2014 Papain-Like Protease (PLpro) Inhibitory Effects of Cinnamic Amides from Tribulus terrestris Fruits. Biol. Pharm. Bull. 37 1021
81. Ghosh A K, Takayama J, Aubin Y, Ratia K, Chaudhuri R, Baez Y, Sleeman K, Coughlin M, Nichols D B and Mulhearn D C 2009 Severe acute respiratory syndrome coronavirus papain-like novel protease inhibitors: design, synthesis, protein-ligand X-ray structure and biological evaluation. J. Med. Chem. 52 5228
82. Cui S and Hao W 2020 Deducing the crystal structure of MERS-CoV helicase. Methods Mol. Biol. 69
83. Jang KJ, Jeong S, Kang D Y, Sp N, Yang Y M and Kim DE 2020A high ATP concentration enhances the cooperative translocation of the SARS coronavirus helicase NSP13 in the unwinding of duplex RNA. Sci. Rep. 10 1
84. Shu T, Huang M, Wu D, Ren Y, Zhang X, Han Y, Mu J, Wang R, Qiu Y and Zhang DY 2020 SARS-Coronavirus-2 NSP13 Possesses NTPase and RNA Helicase Activities That Can Be Inhibited by Bismuth Salts. Virol. Sin. 35 321
85. Zaher N H, Mostafa M I and Altaher A Y 2020 Design, synthesis and molecular docking of novel triazole derivatives as potential CoV helicase inhibitors. Acta Pharm. 70 145
86. Cho J B, Lee J M, Ahn H C and Jeong Y J 2015 A Novel Chemical Compound for Inhibition of SARS Coronavirus Helicase. J. Microbiol. Biotechnol. 27 2070
87. Yu M S, Lee J, Lee J M, Kim Y, Chin Y W, Jee J G, Keum Y S and Jeong Y J 2012 Identification of myricetin and scutellarein as novel chemical inhibitors of the SARS coronavirus helicase, NSP13. Bioorg. Med. Chem. Lett. 22 4049
88. Adedeji A O and Sarafianos S G 2014 Antiviral drugs specific for coronaviruses in preclinical development. Curr. Opin. Virol. 8 45
89. Lee C, Lee J M, Lee N R, Jin B S, Jang K J, Kim D E, Jeong Y J and Chong Y 2009 Aryl diketoacids (ADK) selectively inhibit duplex DNA-unwinding activity of SARS coronavirus NTPase/helicase. Bioorg. Med. Chem. Lett. 19 1636
90. Tanner J A, Zheng B J, Zhou J, Watt R M, Jiang J Q, Wong K L, Lin Y P, Lu L Y, He M L and Kung H F 2005 The adamantane-derived bananins are potent inhibitors of the helicase activities and replication of SARS coronavirus. Chem. Biol. 12 303
91. Kim Y, Jedrzejczak R, Maltseva N I, Wilamowski M, Endres M, Godzik A, Michalska K and Joachimiak A 2020 Crystal structure of NSP15 endoribonuclease NendoU from SARS-CoV-2. Protein Sci. 29 1596
92. Deng X and Baker S C 2018 Coronavirus endoribonuclease is important for evading host antiviral defenses. Virol. J. 517 157
93. Zhang L, Li L, Yan L, Ming Z, Jia Z, Lou Z and Rao Z 2018 Structural and biochemical characterization of endoribonuclease NSP15 encoded by Middle East respiratory syndrome coronavirus. Virol. J. 92 30135128
94. Hackbart M, Deng X and Baker S C 2020 Coronavirus endoribonuclease targets viral polyuridine sequences to evade activating host sensors. Proc. Natl. Acad. Sci. 117 8094
95. Volk A, Hackbart M, Deng X, Cruz-Pulido Y, O'Brien A and Baker S C 2020 Coronavirus endoribonuclease and deubiquitinating interferon antagonists differentially modulate the host response during replication in macrophages. Virol. J. 94 32188729